Research Article   **Open Access**

Jaroslav Hnilica, Lucia Potočňáková, Vít Kudrle*

Time resolved optical emission spectroscopy in power modulated atmospheric pressure plasma jet

Abstract: In this paper, the effects of the power modulation on atmospheric pressure plasma jet, operated in Ar+2%N$_2$ mixture, are studied. Time resolved optical emission spectroscopy is used for the investigation. From line and band intensities, the excitation, vibration and rotation temperatures are calculated. Their evolution during the modulation period exhibits a strong dependence on modulation frequency. For higher modulation frequencies, there is significant discrepancy in rotational temperatures calculated from OH spectra and from N$_2^+$ spectra, which indicates that thermalisation time can reach milliseconds.

1 Introduction

Non-equilibrium low temperature discharges operated at atmospheric pressure are used in a wide range of plasma processing applications, such as plasma surface treatment (cleaning, activation, grafting etc.), plasma enhanced chemical vapour deposition (PECVD) of thin films, plasma decontamination of toxic compounds, and recently in biomedical application and plasma medicine [1-6]. The dielectric barrier discharges (DBD) [1,2] and atmospheric pressure plasma jets (APPJ) [7] belong to the most successful designs. The jet can operate in broad range of the experimental conditions: frequencies from kHz to GHz, discharge dimensions from sub-millimetre to several cm, various gases, and continuous or pulsed regime omit the „are applied". Moreover, the flow regime of plasma jet can enhance the delivery of active species from the active plasma zone to the treated sample. In comparison to the other atmospheric pressure plasma sources the treated surface could be then placed farther [4,8].

Higher average flux of charged particles and significantly lower thermal loading of the treated sample are the main advantages of plasma operating in modulated or pulsed regime over continuous wave (CW) plasma at the same average power. These positive effects result from the non-linear behaviour of the plasma. Moreover, studying the plasma kinetics in modulated and pulsed discharges offer the possibility to understand the mechanisms and processes involved from a fundamental point of view. Plentiful articles have already been published on plasma kinetics of active species in plasma, using time resolved measurements [9-13].

Since in many atmospheric plasma applications the gas temperature has a crucial role, its accurate measurement is very important to optimise the process performance. Investigating the gas temperature (T_{gas}) along with vibrational temperature (T_{vib}) in the pulsed discharge is of particular interest since the plasma chemistry is governed by both of them. There exist well established molecular species (OH, nitrogen, etc.) which are usually used to determine the rotational temperature (T_{rot}) from emission spectra using Boltzmann plot technique. However, the assumption $T_{gas} = T_{rot}$ is valid only under certain conditions. At atmospheric pressure, the collision frequency is high and so these conditions are often considered as easily fulfilled.

This work focuses on atmospheric pressure microwave plasma jet and, instead of simple on-off pulsation, the excitation power is continuously modulated by sinusoidal waveform. The application potential of such design was tested in other works [8,14,15]. The paper continues in the direction of our previous work [16], where the pure argon discharge was investigated, by adding a nitrogen admixture to the argon gas. Using variable modulation frequency, it is possible to study the response of excitation, vibration

*Corresponding author: Vít Kudrle: Masaryk University, Department of Physical Electronics Kotlářská 2, CZ-61137 Brno, Czech Republic, E-mail: kudrle@sci.muni.cz
Jaroslav Hnilica, Lucia Potočňáková: Masaryk University, Department of Physical Electronics Kotlářská 2, CZ-61137 Brno, Czech Republic

and rotation temperatures during the modulation period. The assumption $T_{gas} = T_{rot}$ is investigated using two different spectral systems (OH 306 nm, N_2^+ 391 nm).

2 Experimental Procedure

Fig. 1 shows a schematic drawing of the plasma source. The microwave generator (SAIREM type GMP 20 KED) working on industrial frequency 2.45 GHz has been operated in amplitude modulated (AM) mode. The mean power was set to 250 W (150 W minimum and 350 W maximum). A sinus envelope was used for the modulation. The generator was coupled via a waveguide, ferrite circulator and coaxial cable to the surface wave launcher – surfatron (SAIREM Surfatron 80 with integrated matching) [17]. The reflected power was maintained below 10 W. The surfatron design consists of a coaxial resonant cavity with adjustable wave launching gap, which was typically set under 1 mm. The discharge tube going through the cavity was made from a fused silica and had 170 mm in length while its inner and outer diameter was 1.5 mm and 4 mm, respectively. The end of the discharge tube was placed 2 cm downstream from the surfatron launching gap.

The flow of working gas, argon, was set at 1.45 standard litre per minute (slm) by a flow controller. The nitrogen admixture (2% of argon flow) could be added into the main inlet upstream from the discharge and set by another flow controller. The surfatron cavity, the circulator and the generator were water cooled and the fused silica discharge tube was cooled by a compressed air. The room temperature was 23°C and relative air humidity was 47–56%.

The optical emission spectroscopy was done using a Jobin-Yvon Horiba FHR1000 spectrometer (1.0 m focal length, Czerny-Turner type, 2400 grooves/mm grating, Andor IStar 720 ICCD camera, specified spectral resolution 8 pm, time resolution in order of nanoseconds). A tungsten halogen lamp was used to determine the relative spectral sensitivity of the spectrometer in 200–750 nm range. The light was collected from the whole diameter of the discharge by optic fibre, which was placed perpendicularly to the plasma axis and 2 mm downstream from the discharge tube end. The time-integrated measurements were used for overview emission spectra (the range 275–750 nm) at several AM frequencies. The time-resolved (in synchronisation with the modulation envelope) measurements were used for detailed studies of the Ar I lines, N_2, N_2^+ and OH bands.

3 Results and Discussion

All the measurements were carried out under same operational conditions i.e. same mean power, gas flow rates, optical fibre position, etc., except the changes in AM frequency. The choice of five representative AM frequencies (CW, 80, 800, 1697 and 2459 Hz) was chosen based on our previous studies [8,16,18].

3.1 Overview spectra

The amount of nitrogen admixture (2%) was chosen to be sufficiently high to significantly influence the plasma compared to the pure Ar case [16], but also to be below the limit when the nitrogen admixture would extinguish the discharge. The time-integrated overview emission spectra were recorded in the range (275–750 nm) for several AM frequencies and they are shown in Fig. 2. The spectra are dominated by a molecular band belonging to OH system, by argon atomic lines and by strong emissions from NH system ($A^3\Pi^+ \rightarrow X^3\Sigma$, 336 nm). Another prominent spectral feature is the second positive system of nitrogen ($C^3\Pi_u \rightarrow B^3\Pi_g$), especially the bands corresponding to the vibrational transitions 0-0 (bandhead at 337.1 nm), 1-0 (315.9 nm), 0-1 (357.7 nm) and 0-2 (380.4 nm). In its vicinity, there is the first negative system of nitrogen ion
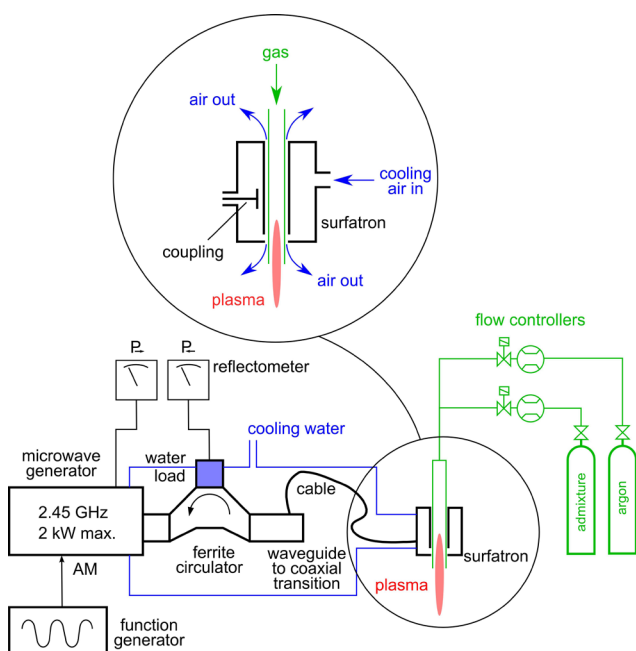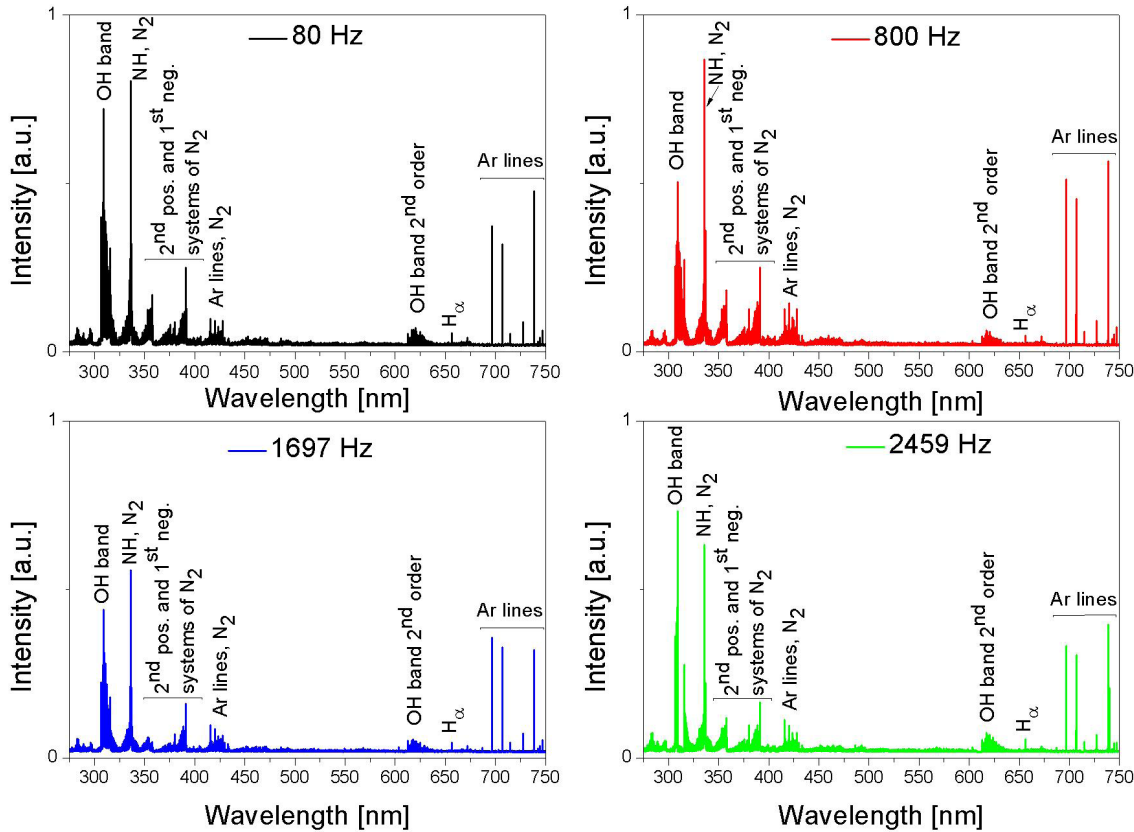

Figure 1: Schematic drawing of the experimental setup.

Figure 2: Overview emission spectra 2 mm outside the discharge tube of atmospheric plasma jet operating in Ar+2%N$_2$ mixture subjected to power modulation by 80, 800, 1697 and 2459 Hz sinus. The spectra were not corrected by spectral sensitivity of the spectrometer.

($B^2\Sigma_u^+ \rightarrow X^2\Sigma_g^+$) at 391.4 nm. Weak bands of second order of OH system (610–630 nm) and H$_\alpha$ line (656 nm) are observable, too. The OH, NH and H are coming from mixing of Ar+N$_2$ plasma with the surrounding air, as OES measurements are carried out outside the discharge tube. However, neither the first positive system of nitrogen nor NO bands are observed in the emission spectra.

Fig. 2 reveals that for 80 and 1697 Hz of the AM, the spectra are almost identical. For 800 Hz, there is significant difference between the intensity of OH system and bandhead (337.1 nm) of the second positive system of nitrogen. For the highest AM frequency (2459 Hz) the emission intensities are reversed and the OH system is more intensive then the nitrogen band. This can be attributed to increased mixing of the plasma effluent with the surrounding air caused by strong coupling between AM frequency and acoustic eigenfrequency of the discharge tube [16].

It should be noted that optical emission spectroscopy cannot fully determine the composition of the plasma as some species can be in the ground state or their emission lines (or bands) are outside the observed wavelength range.

3.2 Excitation temperature estimated from Ar I lines

Electron temperature (T$_e$) is one of the most important plasma parameter but it is difficult to be measured directly. It corresponds to the energy of the plasma electrons and it is important in the ionisation and excitation processes that take place in the discharge. The often used assumption of partial Local Thermodynamic Equilibrium (pLTE) means that top atomic levels obey the Saha equation and Boltzmann statistics. In that case the excitation temperature (T$_{exc}$) derived from the Boltzmann plot [19] should be equivalent to the electron temperature [20-22]. Some authors [23] have used a direct but experimentally challenging technique of Thomson scattering to determine the electron temperature. Their results in a similar plasma jet were around 1.5 to 2 eV. In further, we will discuss only the observable quantity – T$_{exc}$. The evolution of T$_{exc}$ during two AM periods is shown in Fig. 3 and was calculated from the time-resolved and multiply accumulated intensities of selected Ar I lines, Table 1. This particular selection have been used also by other investigators [20,24].

For 80 Hz AM, the T_{exc} is in the range 3600 – 4000 K, with statistical error ± 250 K. This is nearly the same as measured for pure argon plasma in [16]. However, the excitation temperature does not follow the sinusoidal modulation envelope and neither does the statistical error. For 800 Hz modulation, the excitation temperature starts to follow the sinusoidal AM envelope and its statistical error is affected as well. In the maximum, the T_{exc} is (4500 ± 350) K and the statistical error temporarily rises from 6% to 8%. For 1697 Hz modulation, the excitation temperature closely follows the AM envelope and oscillates between (4500 ± 400) K in the minimum and (6700 ± 1100) K in the maximum. The statistical error is also affected where the T_{exc} maximum is two times higher than in the minimum.

The general tendency is essentially the same as in our previous article [16] dealing with pure Ar plasma. The Boltzmann statistics, as expressed by the Boltzmann plot used to calculate the temperature, is valid almost everywhere except the 800 Hz and 1697 Hz modulation maxima. At these points, the fit of Boltzmann model to experimental data produces large statistical error of temperature. For 2459 Hz AM, the calculation of the excitation temperature was not possible due to the excessive noise in the recorded spectra, especially in the range of 400–435 nm and 540–565 nm. The T_{exc} was also determined for CW operation. The excitation temperature was (3872 ± 161) K which corresponds to the mean excitation temperature for 80 Hz AM.

The observed effect that T_{exc} does not follow the AM modulation for low AM frequency (80 Hz) but it does for higher ones (800 and 1697 Hz) is particularly counter-intuitive and needs further investigation.

3.3 Vibrational temperature determined from 2nd positive system of nitrogen

Vibrational temperatures (T_{vib}) is of fundamental importance in plasma processes since the vibrational excitation due to its adiabatic character can trap energy and plays the role of energy reservoir, which is important for chemical reactions in plasma [25]. Moreover, the dissociation of molecules (and thus formation of very reactive atomic radicals) is often governed by step-wise vibrational excitation.

The T_{vib} of molecular nitrogen can be determined using the 2nd positive system of a nitrogen emission spectrum [26]. This implies the electronic transition $C^3\Pi_u \rightarrow B^3\Pi_g$. The sequence with the vibrational quantum

Table 1: List and characteristics of the argon spectral lines used in determining the excitation temperature through a Boltzmann plot.

λ [nm]	E_{q1} [cm^{-1}]	g_q	A_{qp} [10^8 s^{-1}]	Transition
415.9	117 184	5	0.014 00	5p - 4s
416.4	117 151	3	0.002 88	5p - 4s
418.2	118 460	3	0.005 61	5p - 4s
419.8	117 563	1	0.025 70	5p - 4s
420.1	116 943	7	0.009 67	5p - 4s
425.9	118 871	1	0.041 50	5p - 4s
426.6	117 184	5	0.003 33	5p - 4s
427.2	117 151	3	0.008 40	5p - 4s
430.0	116 999	5	0.003 94	5p - 4s
433.4	118 469	5	0.006 00	5p - 4s
433.5	118 460	3	0.003 80	5p - 4s
434.5	118 407	3	0.003 13	5p - 4s
549.6	123 653	9	0.017 60	6d - 4p
555.9	122 087	5	0.014 80	5d - 4p
560.7	121 933	3	0.022 90	5d - 4p
641.6	119 683	5	0.012 10	6s - 4p
667.7	108 723	1	0.002 36	4p' - 4s
675.3	118 906	5	0.020 10	4d - 4p
696.5	107 496	3	0.067 00	4p - 4s
706.7	107 290	5	0.039 50	4p - 4s
714.7	107 132	3	0.065 00	4p' - 4s
727.3	107 496	3	0.020 00	4p' - 4s

number difference $\Delta v = v' - v'' = -2$ was the most intensive and so it was chosen for calculation of the vibrational temperature T_{vib} of N$_2$(C) state. Due to the noise, it was possible to measure intensities just of the three heads of the vibrational sequence: 0-2 at 380.49 nm, 1-3 at 375.54 nm and 2-4 at 371.05 nm, Table 2.

For 80 Hz AM, the time-resolved vibrational temperature (Fig. 4) varies in the range 3300–5000 K with statistical error 100–1000 K without any observable resemblance to the sinusoidal envelope. For 800 Hz, the vibrational temperature increased to 3300–7000 K while statistical error increased to 200–3000 K. Some data points with very bad Boltzmann fit were omitted from the 800 Hz graph. Nevertheless, even remaining data points have quite high statistical error which signifies that the assumption of Boltzmann statistics is generally not valid and that vibrational states are not in thermal equilibrium. The time-resolved spectra for 1697 and 2459 Hz of AM were not suitable for the calculation due to the high noise.
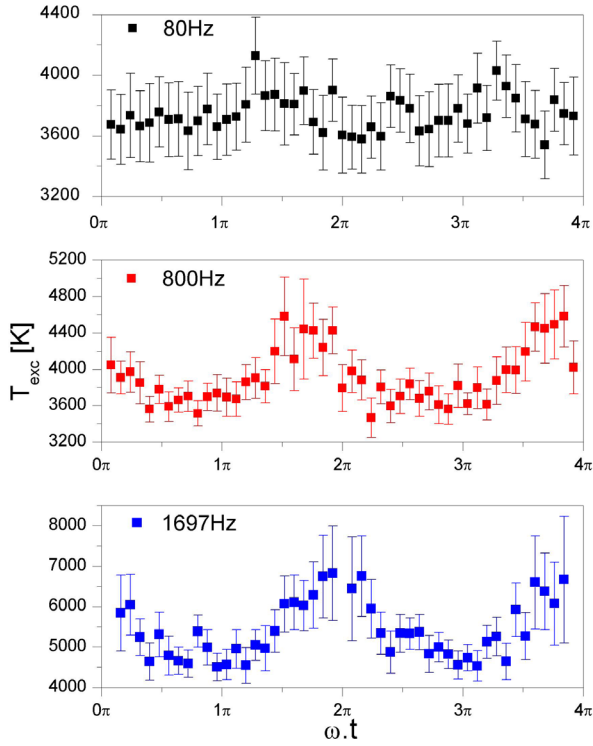
Figure 3: Time-resolved excitation temperature 2 mm outside the discharge tube calculated from Ar I lines for three AM frequencies.
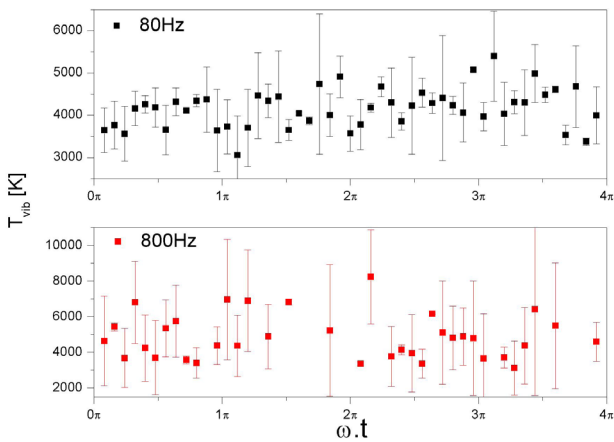
Figure 4: Time-resolved vibrational temperature of $N_2(C)$ state 2 mm outside the discharge tube calculated from 361-380 nm nitrogen band.

The vibrational temperature calculated from the time-integrated and multiple accumulated intensities for 250 W CW power is (4700 ± 500) K which is not only higher than the T_{vib} for 80 Hz AM, but it is also higher than excitation temperature for CW, 80 Hz AM and 800 Hz AM. This suggests that the discharge is in strong deviation from

Table 2: List and characteristics of the nitrogen unresolved band heads used in determining the vibrational temperature using a Boltzmann plot. Transition $C^3\Pi_u \rightarrow B^3\Pi_g$, sequence $\Delta v = v' - v'' = -2$ [26, 27, 28].

| λ [nm]	E [cm⁻¹]	A [10⁶ s⁻¹]	sequence
371.05	4981.00	4.04	2-4
375.54	3012.22	4.93	1-3
380.49	1013.28	3.56	0-2

equilibrium, in which considerable amounts of energy could be stocked in high vibrational levels.

3.4 Rotational temperature calculated from OH (A-X) system and N_2^+ band

The gas temperature is usually estimated from rotational temperature of some molecular species present in the discharge such as OH [24,29-32], N_2^+ [33,34], CN [35] or C_2 [36] on account of the highly favourable energy exchange between heavy particles and the internal rotational-vibrational states of the molecular species involved [37]. Assuming that admixture molecules are in equilibrium with the gas atoms majority, the rotational temperature (T_{rot}) derived from the ro-vibrational spectra can be considered equal to the gas temperature (T_{gas}) [28].

Such an assumption had already been used with N_2 in argon gas at pressures exceeding typically 10 kPa [38]. Authors of [39] have utilised N_2^+, N_2, CN and OH as thermometric species in an argon microwave discharge at atmospheric pressure. They found that the value of T_{rot} from N_2^+, N_2, and CN agreed within experimental error, and that the OH band was a reliable thermometer for $T_{gas} < 1800$ K [20,39].

In this paper, the T_{rot} was calculated using the intensities of particular selection of OH lines (Table 3) which was used also by other authors [20,30,40]. The time-resolved rotational temperatures are shown in Fig. 5. The behaviour of the T_{rot} for 80 Hz AM follows the sinusoidal AM signal. It oscillates synchronously with the power envelope between (2100 ± 500) K and (2850 ± 500) K, so the statistical error is around 25%. Typical Boltzmann plots used for the calculation are shown in Fig. 6. Rotational Boltzmann statistics is valid just for the lower parts of the temperature curve for 80 Hz of AM. It is the same for 800 Hz of AM, nevertheless the temperature does not follow the sinusoidal envelope. It seems that for the temperatures with high errors, the rotational levels of the OH(A) state do not follow a Boltzmann distribution, so it is
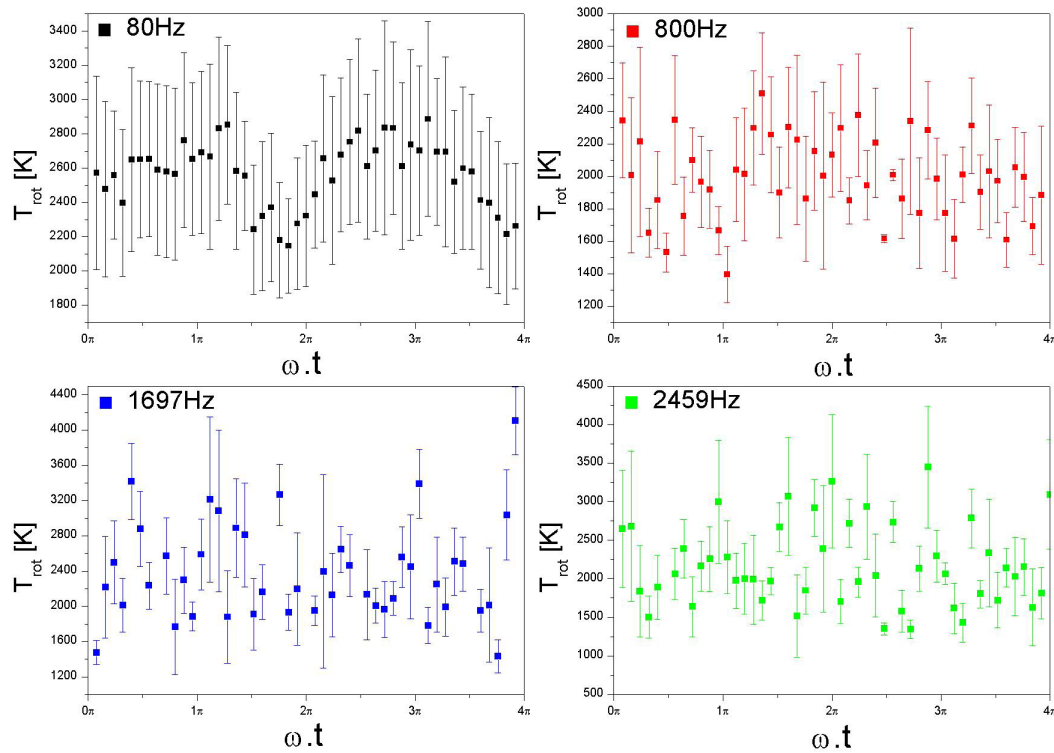
Figure 5: Time-resolved rotational temperature 2 mm outside the discharge tube calculated from OH (A-X) system for four AM frequencies.

not possible to directly infer the translational temperature of the gas from the OH(A-X) measurement. The discharge is probably in a strongly non-equilibrium state. Or simply, using this band is not suitable for temperature estimation when the power is amplitude modulated.

For the other modulation frequencies, the rotational temperature in Ar+N_2 plasma is not able to follow the varying incident power. Together with the statistical error, it is changing virtually randomly and independently of the AM envelope. This effect has the same principal cause as the non-equilibrium itself – slow energy cascade from the electronic excitations to rotations and/or translations.

The T_{rot}(OH) calculated for the CW input power is (2995 ± 168) K. It is higher temperature than in the maximum for 80 Hz AM. This means that simply using AM (at least in the case for 80 Hz) instead of CW in Ar+N_2 plasma significantly decreases the T_{gas}. This could be very useful for surface plasma treatment of heat sensitive materials.

In principle, the gas temperature can be determined using any molecular rotational band. As the nitrogen spectral bands (Fig. 2) were recorded with sufficient intensity and resolution, one may use [26] either the first negative system at 391.4 nm or second positive system bands at 337.4 or 380.4 nm. In this paper, it was chosen

Table 3: List and parameters of the selected OH spectral lines used for determining the rotational temperature using a Boltzmann plot.

Line	λ [nm]	E [cm⁻¹]	A [10⁸ s⁻¹]
Q_1(9/2)	308.3278	32.779	33.7
Q_1(11/2)	308.5196	32.948	42.2
Q_1(13/2)	308.7338	33.150	50.6
Q_1(17/2)	309.2394	33.652	67.5
Q_1(19/2)	309.5324	33.952	75.8
Q_1(21/2)	309.8586	34.283	84.1

Table 4: Lines from the *P*-branch of the 1st negative system of the N_2^+ and their characteristic parameters used to calculate the rotational temperature.

λ [nm]	A	B	λ [nm]	A	B
391.25	44	462	390.76	60	870
391.15	48	552	390.60	64	992
391.04	52	650	390.41	68	1122
390.91	56	756			
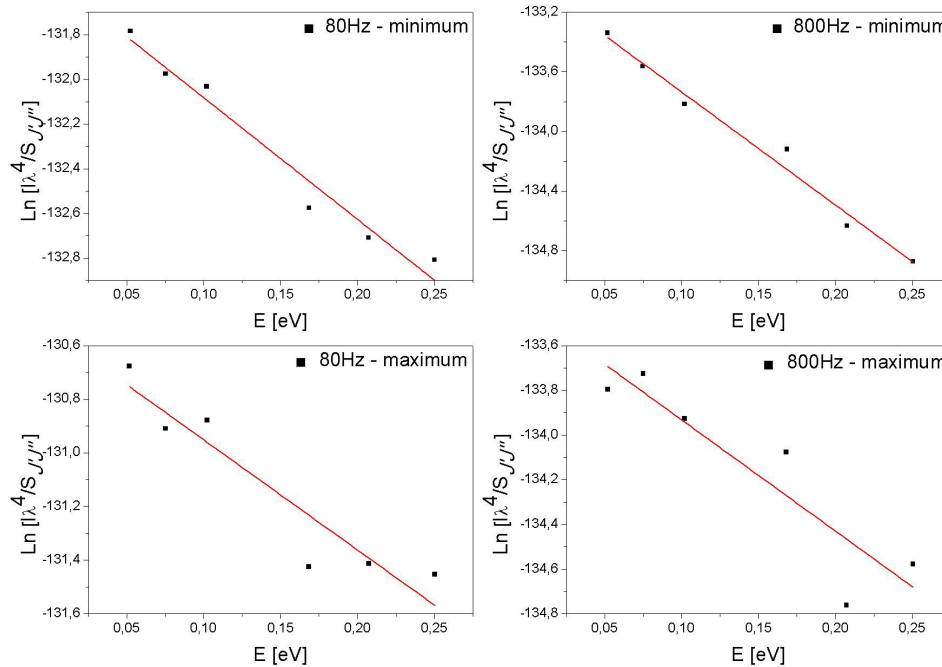
Figure 6: The selected Boltzmann plots used for calculation of OH rotational temperature in Fig. 5. The graphs are shown for (top left) 80 Hz and $\omega t = 1.84\pi$, (top right) 800 Hz and $\omega t = 0.48\pi$, (bottom left) 80 Hz and $\omega t = 2.72\pi$, and (bottom right) 1697 Hz and $\omega t = 2.72\pi$.
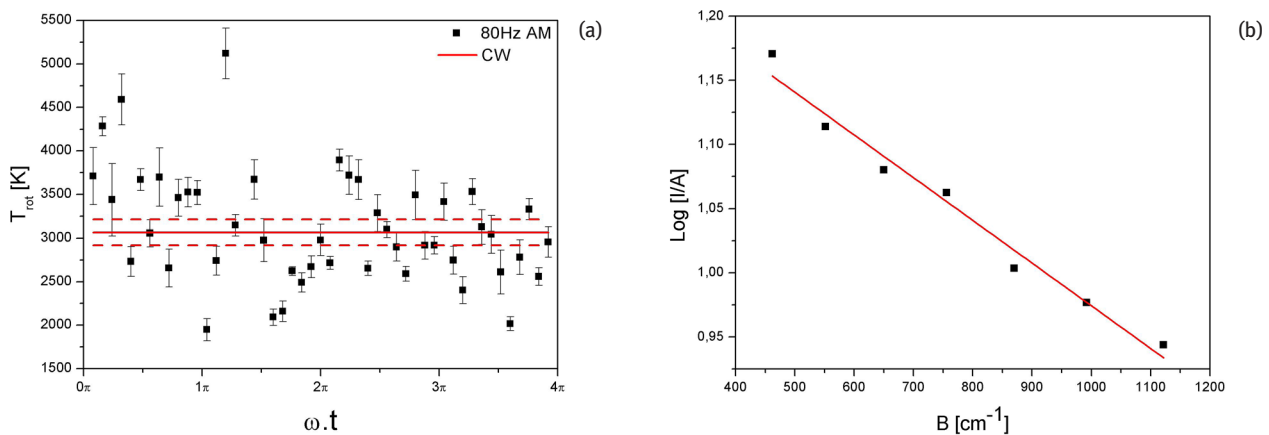
Figure 7: On the left, there is time-resolved rotational temperature 2 mm outside the discharge tube calculated from 1st negative system of nitrogen for 80 Hz AM. The results for CW excitation are shown, too. On the right, there is a typical Boltzmann plot used for a calculation of the temperature ($\omega t = 2.16\pi$).

to calculate the T_{rot} from N_2^+ transition ($B^2\Sigma_u^+ \rightarrow X^2\Sigma_g^+$) (0-0) at 391.4 nm. From relative intensities (I), T_{rot} could be obtained on the assumption of a Boltzmann distribution for rotational-vibrational levels from the slope of equation $\log(IA^{-1}) = -(1.296\, T_{rot}^{-1})\, B$, where parameters A and B are specific for each rotational transition (Table 4) [41].

The time-resolved rotational temperature calculated from the 1st negative system of the N_2 for 80 Hz AM is presented in Fig. 7 together with one typical Boltzmann plot. The rotational temperature is in the range of 1900–4300 K with the statistical error mostly below 10%, i.e. ± 250 K. The points seem to be virtually random and do not resemble the sinusoidal AM envelope. The time-resolved spectra for other AM frequencies were not suitable for the calculation due to the high noise. The rotational temperature calculated for the CW case is (3067 ± 148) K and it is in the middle of the temperature range for 80 Hz of AM (Fig. 7).

It is clear that in the power modulated plasma, the T_{rot} calculated from 1st negative system of the N_2^+ and T_{rot} calculated from OH (A-X) system are not compatible. The 1st negative system does not react even to 80 Hz modulation. It then follows that equilibrium between rotations and translations is not established even after 10 ms. Discrepancies between rotational temperature of OH and N_2 have been also reported in vapour-air bubbles in liquids [42,43] and in the near electrode region of at atmospheric pressure glow discharges with liquid electrodes [44-46].

However, the results for CW power – (2995 ± 168) K from OH and (3067 ± 148) K from N_2^+ agree within the experimental error not only mutually, but also with paper [39].

4 Conclusions

The time-resolved optical emission spectroscopy was used to investigate the influence of the power modulation on microwave atmospheric pressure plasma jet operating in Ar +2%N_2 mixture. Instead of classical on-off pulsation, the continuous, sinusoidal power envelope was used.

The excitation temperature, calculated from Ar I lines, increases with the modulation frequency. It follows the sinusoidal AM envelope very well for higher AM frequency (800 and 1697 Hz) but not for 80 Hz.

The vibrational temperature calculated from the 2nd positive system of nitrogen does not follow the modulation envelope and seems to be rather constant during AM period. Stronger deviations from Boltzmann statistics were observed for higher AM frequencies.

In the case of CW power, the rotational temperatures, determined from OH and N_2^+ bands, agree quite well. This explains why both OH and N_2^+ are recommended as thermometric species in many works. However, this agreement disappears when the plasma is power modulated. The N_2^+ rotations do not follow the modulation at all. The OH rotational temperature is able to follow the 80 Hz modulation. Using 80 Hz AM instead of CW in Ar+N_2 plasma seems to significantly decrease the T_{gas}, which could be of importance for many applications.

For higher modulation frequencies, the assumption of rotational Boltzmann statistics is not fulfilled. So, despite the high collision rate and consequently fast thermalisation in atmospheric pressure plasmas, the rotational equilibrium is established rather slowly, after 10 ms. This should be taken into account in all experiments trying to estimate the gas temperature from rotational spectra.

References

[1] Kogelschatz U., Dielectric-barrier discharges: Their history, discharge physics and industrial applications, Plasma Chem. Plasma Process., 2003 23, 1-46.

[2] Wagner H.E., Brandenburg R., Kozlov K.V., Sonnenfeld A., Michel P., Behnke J.F., The barrier discharge: Basic properties and applications to surface treatment, Vacuum, 2003, 71, 417-436.

[3] Shenton M.J., Stevens G.C., Surface modification of polymer surfaces: atmospheric plasma versus vacuum plasma treatments, J. Phys. D: Appl. Phys., 2001, 34, 2761.

[4] Schafer J., Foest R., Quade A., Ohl A., Weltmann K.-D., Local deposition of SiOx plasma polymer films by a miniaturized atmospheric pressure plasma jet (APPJ), J. Phys. D: Appl. Phys., 2008. 41, 194010.

[5] Lee J.K., Kim M.S., Byun J.H., Kim K.T., Kim G.C., Park G.Y., Biomedical Applications of Low Temperature Atmospheric Pressure Plasmas to Cancerous Cell Treatment and Tooth Bleaching, Jap. Jour. Appl. Phys., 2011, 50, 08JF01.

[6] Weltmann K.-D., Polak M., Masur K., von Woedtke T., Winter J., Reuter S., Plasmas processes plasma sources in medicine, Contrib. Plasma Phys., 2012, 52, 644-654.

[7] Babayan S.E., Jeong J.Y., Tu V.J., Park J., Selwyn G.S., Hicks R.F., Deposition of silicon dioxide films with an atmospheric-pressure plasma jet, Plasma Sources Sci. Technol., 1998, 7, 286-288.

[8] Hnilica J., Schafer J., Foest R., Zajickova L., Kudrle V., PECVD of nanostructured SiO2 in a modulated microwave plasma jet at atmospheric pressure, J. Phys. D: Appl. Phys., 2013, 46, 335202.

[9] Lieberman M.A., Lichtenberg A.J., Principles of Plasma Discharges and Materials Processing, 2nd ed., Wiley Interscience, Hoboken, 2005.

[10] Behle S., Brockhaus A., Engemann J., Time-resolved investigations of pulsed microwave-excited plasmas, Plasma Sources Sci. Technol., 2000, 9, 57-67.

[11] Rousseau A., Teboul E., Sadeghi N., Time resolved gas temperature measurements by laser absorption in a pulsed microwave hydrogen discharge, Plasma Sources Sci. Technol., 2004, 13, 166-176.

[12] Britun N., Godfroid T., Konstantinidis S., Snyders R., Time-resolved gas temperature evolution in pulsed Ar–N2 microwave discharge, Appl. Phys. Lett., 2011, 98, 141502.

[13] van der Horst R.M., Verreycken T., van Veldhuizen E.M., Bruggeman P., Time-resolved optical emission spectroscopy of nanosecond pulsed discharges in atmospheric-pressure N2 and N2/H2O mixtures, J. Phys. D: Appl. Phys., 2012 45, 345201.

[14] Potocnakova L., Hnilica J., Kudrle V., Increase of wettability of soft- and hardwoods using microwave plasma, Int. J. Adh. Adh., 2013, 45, 125-131.

[15] Hnilica J., Potocnakova L., Stupavska M., Kudrle V., Rapid surface treatment of polyamide 12 by microwave plasma jet, Appl. Surf. Sci., 2014, 288, 251-257.

[16] Hnilica J., Kudrle V., Time-resolved study of amplitude modulation effects in surface-wave atmospheric pressure argon plasma jet, J. Phys. D: Appl. Phys., 2014, 47, 085204.

[17] Moisan M., Beaudry C., Leprince P., A new HF device for the production of long plasma columns at a high electron density, Physics Letters, 1974, 50A, 125-126.

[18] Hnilica J., Kudrle V., Potocnakova L., Surface treatment by atmospheric-pressure surfatron Jet, IEEE Trans. Plasma Sci., 2012, 40, 2925-2930.

[19] Griem H.R., Plasma spectroscopy, McGraw-Hill, New York, 1964.

[20] Calzada M.D., Moisan M., Gamero A., Sola A., Experimental investigation and characterization of the departure from local thermodynamic equilibrium along a surface-wave-sustained discharge at atmospheric pressure, J. Appl. Phys., 1996, 80, 46-55.

[21] Van der Mullen J.A.M., Excitation equilibria in plasmas; a classification, Phys. Rep. 1990, 191, 109-220.

[22] Sainz A., Margot J., Garcia M.C., Calzada M.D., Role of dissociative recombination in the excitation kinetics of an argon microwave plasma at atmospheric pressure, J. Appl. Phys., 2005, 97, 113305.

[23] van Gessel A.F.H., Carbone E.A.D., Bruggeman P.J., van der Mullen J.J.A.M., Laser scattering on an atmospheric pressure plasma jet: disentangling Rayleigh, Raman and Thomson scattering, Plasma Sources Sci. Technol., 2012, 21, 015003.

[24] Calzada M.D., Garcia M., Luque J.M., Santiago I., Influence of the thermodynamic equilibrium state in the excitation of samples by a plasma at atmospheric pressure, J. Appl. Phys., 2002, 92, 2269-2275.

[25] Fridman A., Kennedy L.A., Plasma Physics and Engineering, Taylor & Francis, London, 2004.

[26] Popa S.D., Vibrational distributions in a flowing nitrogen glow discharge, J. Phys. D: Appl. Phys. 1996, 29, 411-415.

[27] Herzberg G., Molecular Spectra and Molecular Structure I. Spectra of Diatomic Molecules, 2nd ed., Litton Educational Publ., Inc., New York, 1950.

[28] Lofthus A., Krupenie P.H., The spectrum of molecular nitrogen, J. Phys. Chem. Ref. Data, 1997, 6, 113-307.

[29] Garcia M.C., Yubero C., Calzada M.D., Martinez-Jimenez M.P., Spectroscopic characterization of two different microwave (2.45 GHz) induced argon plasmas at atmospheric pressure, Appl. Spectrosc., 2005, 59, 519-528.

[30] Munoz J., Dimitrijevic M.S., Yubero C., Calzada M.D., Using the van der Waals broadening of spectral atomic lines to measure the gas temperature of an argon–helium microwave plasma at atmospheric pressure, Spectrochim. Acta Part B, 2009, 64, 167-172.

[31] Meinel H., Krauss L., Über die besetzung der rotationszustände von oh und C2 in niederdruckplasmen, J. Quant. Spectr. Radiat. Transfer., 1969 9, 443-460.

[32] Christova M., Castanos-Martinez E., Calzada M.D., Kabouzi Y., Luque J.M., Moisan M., Electron density and gas temperature from line broadening in an argon surface-wave-sustained discharge at atmospheric pressure, Appl. Spectrosc., 2004, 58(9), 1032-1037.

[33] Munoz J., Margot J., Calzada M.D., Experimental study of a helium surface-wave discharge at atmospheric pressure, J. Appl. Phys., 2010, 107, 083304.

[34] Rodero A., Quintero M.C., Sola A., Gamero A., Preliminary spectroscopic experiments with helium microwave induced plasma produced in air by use of a new structure: the axial injection torch, Spectrochim. Acta Part B, 1996, 51, 467-479.

[35] Cruden B.A., Rao M.V.V.S., Sharma S.P., Meyyappan M., Neutral gas temperature estimates in an inductively coupled CF4 plasma by fitting diatomic emission spectra, J. Appl. Phys., 2002, 91, 8955-8964.

[36] Lombardi G., Benedic F., Mohasseb F., Hassouni K., Gicquel A., Determination of gas temperature and C2 absolute density in Ar/H2/CH4 microwave discharges used for nanocrystalline diamond deposition from the C2 Mulliken system, Plasma Sources Sci. Technol., 2004, 13, 375-386.

[37] Mermet J., Inductively coupled plasma emission spectrometry, Part II: Applications and Fundamentals, Wiley-Insterscience, New York, 1987

[38] Moussounda P.S., Ranson P., Mermet J.M., Spatially resolved spectroscopic diagnostics of argon MIP produced by surface wave propagation (Surfatron), Spectrochim. Acta B, 1985, 40, 641-651.

[39] Ricard A., St-Onge L., Malvos H., Gicquel A., Hubert J., Moisan M., Torche a plasma a excitation micro-onde : deux configurations complémentaires, J. Phys. III, 1995, 5, 1269-1285.

[40] Gavare Z., Svagere A., Zinge M., Revalde G., Fyodorov V., Determination of gas temperature of high-frequency low-temperature electrodeless plasma using molecular spectra of hydrogen and hydroxyl-radical, J. Quant. Spectrosc. Radiat. Transfer, 2012, 113, 1676-1682.

[41] Rincon R., Munoz J., Saez M., Calzada M.D., Spectroscopic characterization of atmospheric pressure argon plasmas sustained with the Torche a Injection Axiale sur Guide d'Ondes, Spectrochim. Acta Part B, 2013, 81, 26-35.

[42] Bruggeman P., Schram D.C., Gonzalez M.A., Rego R., Kong M.G., Leys C., Characterization of a direct dc-excited discharge in water by optical emission spectroscopy, Plasma Sources Sci. Technol., 2009, 18, 025017.

[43] Bruggeman P., Degroote J., Vierendeels J., Leys C., Plasma characteristics in air and vapor bubbles in water, In: J. Schmidt, M. Simek, S. Pekarek, V. Prukner (Ed.), Proceedings of 28th International Conference on Phenomena in Ionized Gases (15-20 July 2007, Prague, Czech Republic), Institute of Plasma Physics AS CR Prague, 2007, 859-862.

[44] Mezei P., Cserfalvi T., Csillag L., The spatial distribution of the temperatures and the emitted spectrum in the electrolyte cathode atmospheric glow discharge, J. Phys. D.: Appl. Phys., 2005, 38, 2804.

[45] Mezei P., Cserfalvi T., Electrolyte cathode atmospheric glow discharges for direct solution analysis, Appl. Spectrosc. Rev., 2007, 42, 573-604.

[46] Mezei P., Cserfalvi T., A critical review of published data on the gas temperature and the electron density in the electrolyte cathode atmospheric glow discharges, Sensors, 2012, 12, 6576-6586.